Online at www.sciencemag.org/cgi/content/full/295/5556/838/DC1.
7. J. P. Peixoto, A. H. Oort, *Physics of Climate* (American Institute of Physics, New York, 1992).
8. Anomalies are defined as the deviation from the mean annual cycle for the years 1985–1993.
9. The commonly used NINO3 ENSO index is defined as the 150°W–90°W 5°S–5°N average sea surface temperature anomaly.
10. M. Chelliah, P. Arkin, *J. Clim.* **5**, 371 (1992).
11. The two-dimensional JFD is a matrix whose elements contain the frequency of occurrence of various pairs of parameter values (in this case, SW and LW fluxes). In this research, all data sets are monthly means and are mapped to 5° × 5° spatial resolution. The JFDs are calculated on the basis of these data sets.
12. The mean annual cycle is calculated from the composite 1985–1993 JFD, and then the JFD anomalies time series is derived. The JFD anomalies matrix is smoothed before EOF decomposition. Through EOF decomposition, we obtain a series of modes arranged in decreasing order of the fractions of variance that they can explain. Each mode has two components: The EOF, the eigenvector of the covariance matrix, represents the JFD pattern of the mode; the PC, the time series of the projection of each month's JFD anomaly on this EOF, represents the temporal variation.
13. W. B. Rossow, R. A. Schiffer, *Bull. Am. Meteorol. Soc.* **80**, 2261 (1999).
14. J. J. Bates, D. L. Jackson, *Geophys. Res. Lett.* **28**, 1695 (2001).
15. J. Hansen, R. Ruedy, J. Glascoe, M. Sato, *J. Geophys. Res.* **104**, 30997 (1999).
16. Omega is the standard meteorological symbol for the vertical velocity in pressure coordinates in units of Pa s^{-1}. Its direction is upward when its value is negative.
17. E. Kalnay *et al.*, *Bull. Am. Meteorol. Soc.* **77**, 437 (1996).
18. The JFD anomalies of the five parameters and LW flux are combined to construct new two-dimensional matrices. After the EOF analysis is applied to the time series of the new matrices, the resulting EOF of each mode is separated back into five individual JFD patterns, one for each parameter and the LW flux. The five JFD patterns share the PC time series together; that is, a given mode depicts related variations in all the parameters and fluxes. As a separate test, we also performed an EOF analysis for each parameter and for LW flux JFD anomalies individually for the entire tropics. The correlations of the resulting PCs with the tropical mean LW anomalies time series are as follows: cloud amount–LW, 0.75; UTH-LW, 0.75; omega-LW, 0.86; and SAT-LW, 0.93.
19. S. Levitus, J. I. Antonov, T. P. Boyer, C. Stephens, *Science* **287**, 2225 (2000).
20. M. Latif, R. Kleeman, C. Eckert, *J. Clim.* **10**, 2222 (1997).
21. D. E. Parker, *Science* **287**, 1216 (2000).
22. S. Power, T. Casey, C. Folland, A. Colman, V. Mehta, *Clim. Dyn.* **15**, 319 (1999).
23. D. J. Gaffen *et al.*, *Science* **287**, 1242 (2000).
24. E. C. Weatherhead *et al.*, *J. Geophys. Res.* **103**, 17149 (1998).
25. Supported by the NASA Tropical Rainfall Measuring Mission and the Department of Energy Atmospheric Radiation Measurement Program. We thank R.-X. Ying, D. Chen, J.-P. Liu, R. A. Ruedy, Y.-C. Zhang, and L. DelValle for their help at various stages of this work; B. A. Wielicki and K.-M. Xu for their comments on the manuscript; and B. A. Wielicki for suggesting the test to confirm that calibration shifts cannot explain the results. The ERBE, CERES, and the International Satellite Cloud Climatology Project data were obtained from the NASA Langley Research Center Atmospheric Sciences Data Center. J. J. Bates and D. L. Jackson provided the HIRS UTH data. The NCEP Reanalysis data are provided by the National Oceanic and Atmospheric Administration–Cooperative Institute for Research in Environmental Sciences Climate Diagnostics Center, Boulder, CO, USA, from their Web site at http://www.cdc.noaa.gov/.

29 August 2001; accepted 18 December 2001

REPORTS

Evidence for Large Decadal Variability in the Tropical Mean Radiative Energy Budget

Bruce A. Wielicki,[1]* Takmeng Wong,[1] Richard P. Allan,[2] Anthony Slingo,[2] Jeffrey T. Kiehl,[3] Brian J. Soden,[4] C. T. Gordon,[4] Alvin J. Miller,[5] Shi-Keng Yang,[5] David A. Randall,[6] Franklin Robertson,[7] Joel Susskind,[8] Herbert Jacobowitz[9]

It is widely assumed that variations in Earth's radiative energy budget at large time and space scales are small. We present new evidence from a compilation of over two decades of accurate satellite data that the top-of-atmosphere (TOA) tropical radiative energy budget is much more dynamic and variable than previously thought. Results indicate that the radiation budget changes are caused by changes in tropical mean cloudiness. The results of several current climate model simulations fail to predict this large observed variation in tropical energy budget. The missing variability in the models highlights the critical need to improve cloud modeling in the tropics so that prediction of tropical climate on interannual and decadal time scales can be improved.

Earth's climate system is driven by a radiative energy balance between the solar or shortwave (SW) radiation absorbed by Earth and the thermal infrared or longwave (LW) radiation emitted back to space. The balance both modifies and is modified by the components of the Earth-atmosphere system such as clouds, the surface, and the atmosphere (*1*). Therefore, the TOA radiation budget is crucial in determining climate variability and feedbacks, whereas its measurement provides a severe test of our ability to represent physical processes important for simulations of future climate.

A new set of Earth radiation balance data is now being provided by the NASA CERES (Clouds and the Earth's Radiant Energy System) instrument on the Tropical Rainfall Measuring Mission (TRMM) for 8 months in 1998 and by the Terra satellite mission that began in March 2000 and is expected to continue through 2007 (*2*, *3*). In addition, with the 16-year record of the Earth Radiation Budget Satellite (ERBS), it is now possible to examine 22 years of accurate satellite observed broadband radiative fluxes (*4*–*6*). Anomalies in tropical mean broadband thermal LW flux emitted by the Earth have been determined from this 22-year record and are shown in Fig. 1.

Calibration absolute accuracies for the seven broadband radiometers in Fig. 1 are estimated to be roughly 1% for the pre-CERES instruments and 0.5% for the newer records. The anomaly results during data overlap periods from all instruments are consistent to within about 1 Wm^{-2} or about 0.5% of the 253 Wm^{-2} ERBE tropical mean LW flux. Only stability of calibration enters the anomaly record for the ERBS nonscanner (NS) data, whereas both stability and absolute calibration affect the scanner (SC) anomaly records from five different instruments.

The LW anomaly record in Fig. 1 shows much larger variations than expected, especially for the 1997/1998 El Niño event, which reaches a tropical mean anomaly of 8 Wm^{-2}, the largest seen to date. Other notable short-term anomalies are the rapid drop in LW flux resulting from the Mount Pinatubo Eruption in 1991 (*7*), followed by the expected 2-year recovery period as the volcanic aerosols are removed from the stratosphere and upper troposphere. Although the 1983 El Niño event is thought to be comparable in magnitude to the 1997/1998 El Niño, there is no comparable tropical mean LW flux anomaly. A plausible hypothesis is that the earlier 1982 El Chichon eruption caused a reduction in LW flux similar to that from the Mount Pinatubo Eruption in 1991. The resulting LW fluxes in 1982 to 1984 would, in this case, be a partial cancellation of the El Chichon and El Niño signals. But the most surprising result in the figure is an apparent drop of about 2 Wm^{-2} in LW

[1]NASA Langley Research Center, Hampton, VA 23681, USA. [2]Hadley Centre, Met Office, Bracknell, RG12 2SY, UK. [3]National Center for Atmospheric Research, Post Office Box 3000, Boulder, CO 80303, USA. [4]GFDL/NOAA, Princeton University, Post Office Box 308, Princeton, NJ 08542, USA. [5]NOAA Climate Prediction Center/NCEP, Camp Springs, MD 20746, USA. [6]Colorado State University, Fort Collins, CO 80523, USA. [7]NASA Marshall Space Flight Center, Huntsville, AL 35812, USA. [8]NASA Goddard Space Flight Center, Greenbelt, MD 20771, USA. [9]NOAA/NESDIS, Camp Springs, MD 20746, USA.

*To whom correspondence should be addressed. E-mail: b.a.wielicki@larc.nasa.gov

flux from the late 1970s to the mid 1980s, followed by a rise of about 4 Wm^{-2} from the late 1980s to the mid to late 1990s. Indeed, if the Pinatubo volcanic reduction from 1991 to 1993 is removed, the tropics appear to undergo an increase in LW flux from 1989 to 1994, followed by a relatively steady value from 1994 through 2001, with the exception of the large 1997/1998 El Niño event.

Because radiative forcings of 1 Wm^{-2} or less are important for climate change prediction, natural variability of 4 Wm^{-2} in the LW part of the tropical radiation budget is considered a major change. The reality of these large changes is supported by the consistency of the results from seven independent broadband radiation instruments, all supporting the same pattern of decadal variability. Though there are two narrow spectral band radiometer sources of LW estimates, these are not considered as accurate as the broadband LW fluxes. The latest versions of these narrowband data sets disagree with each other as well as with the broadband data when used to determine tropical decadal changes in LW flux (*8*). Because the ERBS NS record spans the entire period and includes regular solar constant measurements by both SW and Total channels, we re-examined this record extensively for any potential problems with calibration and found none at levels higher than 0.2 to 0.5 Wm^{-2} (*9*). Therefore, we conclude that it is unlikely that this decadal variability can be explained by instrument calibration changes.

Is this decadal increase of 4 Wm^{-2} a signal of global warming? Certainly, it is not a direct one. The flux changes are far too large to be explained by the small surface and atmosphere warming over this time period, which will tend to be offset by increased CO_2 and water vapor greenhouse gas trapping. This can be demonstrated with the use of CERES scanner data in 1998 and the ERBE scanner data in 1985–1989 used in Fig. 1. These data have sufficiently small fields of view (10 and 40 km, respectively) to allow separation of the data into clear-sky and cloudy-sky regions of the tropics. Recent analysis of the clear-sky scanner LW flux data (*10*) showed that changes during and after the 1998 El Niño were consistent with the observed changes in sea surface temperature (SST) and water vapor. By the end of the El Niño in July 1998, the clear-sky LW fluxes measured by CERES agreed with the ERBE climatological July 1985–1989 average values to within 0.5 Wm^{-2}. The largest anomaly of clear-sky LW fluxes reached only 2 Wm^{-2} during the El Niño peak of February and March 1998, whereas the total anomaly in Fig. 1 reaches about 8 Wm^{-2}. This leaves the factor of 4 to 8 larger anomalies shown in Fig. 1 to be explained by changes in the cloudy-sky conditions in the tropics.

Though 8 Wm^{-2} is large for a clear-sky radiation anomaly, clouds can cause changes of up to 200 Wm^{-2} or larger in both LW emitted and diurnally averaged SW reflected radiation fields for deep, thick clouds in the tropics. The LW-emitted flux changes are caused by cloud increases in greenhouse trapping, whereas SW-reflected flux changes are caused by cloud increases in reflected solar energy. The net radiative effect of clouds is a balance between the LW greenhouse and SW cooling effects.

Figure 2 shows the observed broadband anomalies for LW-emitted, SW-reflected, and net radiation flux changes in the tropics. Aerosols from the Mount Pinatubo eruption cause the large increase in SW-reflected flux in 1991 to 1993. As tropical mean LW-emitted flux increases in the mid to late 1990s, SW-reflected flux decreases. Both effects are consistent with a decrease in tropical cloudiness. Figure 2 also shows evidence of increased seasonal variability. To more clearly isolate these variations in Fig. 2 from El Niño and Mount Pinatubo signals, Fig. 3 shows the average tropical mean LW flux, SW flux, and SW albedo anomaly averaged separately for each seasonal month over the 4-year period 1994 through 1997, which contains the large semi-annual anomalies in SW and Net fluxes. The results show a decrease of more than 0.01 in tropical mean albedo in the spring and fall seasons, but little change in the summer and winter seasons, indicating a changed phasing of seasonal cloudiness in the tropics (*11*). Because Fig. 3 shows that the LW flux increase in 1994 through 1997 is almost constant with season, we further conclude that the seasonal cycle in albedo is likely dominated by changes in low-level cloudiness that have little effect on the LW fluxes but a large impact on the SW fluxes.

The above analysis indicates strong evidence for decadal variations in the radiative balance components in the tropical atmosphere. These changes are sufficiently large that, in principle, they should be seen in climate model predictions. We have tested

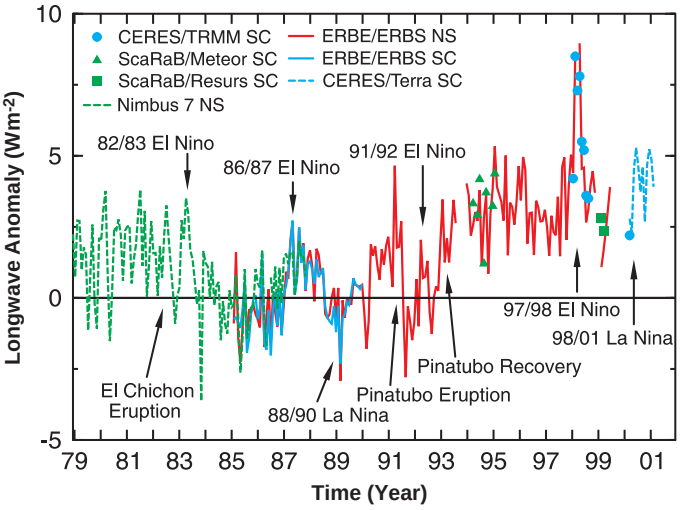

Fig. 1. Satellite record of tropical mean (20°S to 20°N latitude) anomalies in broadband thermal emitted LW flux. Anomalies are referenced to the ERBS scanner baseline period of 1985 through 1989, which most climate models use as a baseline for comparison (*5*). Results are shown from seven different broadband instruments on six spacecraft missions (*6*).

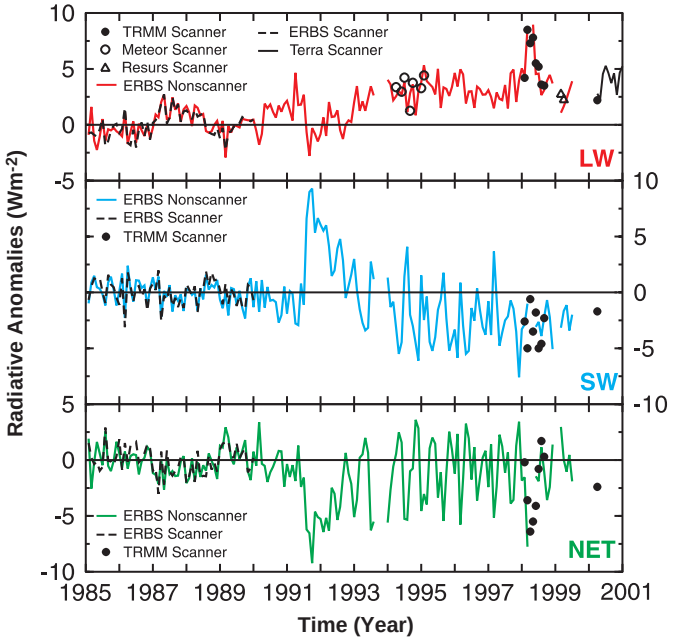

Fig. 2. Satellite record of tropical mean (20°S to 20°N latitude) anomalies in broadband thermal emitted LW flux, solar reflected SW flux, and net radiative flux. Net flux is defined as solar insolation – SW-reflected flux – LW-emitted flux. A smaller set of satellites is shown for SW- and net-radiative flux anomalies. Only those satellites whose orbits systematically sample the entire diurnal cycle in about a month, so the large diurnal cycle of solar reflected fluxes can be accurately determined across the entire tropics (*25*).

this hypothesis by analyzing decadal integrations of the atmospheric model components of four climate models and one weather assimilation model, forced by the observed SSTs (*12*) for the 1985 through 1998 period. The integrations ignore the effects of volcanic aerosols. The climate models include the Hadley Centre atmospheric climate model HadAM3 (*13*, *14*), the National Center for Atmospheric Research (NCAR) model CCM3 (*15*), the Geophysical Fluid Dynamics Laboratory (GFDL) Climate Model (*16*), and the GFDL EP (Experimental Prediction) model (*17*). We also included the National Center for Environmental Prediction (NCEP)–NCAR 50-Year Reanalysis, which uses the NCEP 4-D Assimilation Model (*18*). For all model runs, the tropical mean anomalies were calculated as in the satellite data, using the 1985 through 1989 period as the baseline.

Figure 4 compares the atmospheric model results to the ERBS NS satellite observations presented in Fig. 2. There is remarkably little variation in the tropical mean fluxes from the models when compared to the data. Even near the peak of the 1997/1998 El Niño event, in early 1998, the tropical mean model response is only about one-third that of the observations.

No significant decadal variability is exhibited by the climate and reanalysis models. Correlation coefficients of the observed and modeled tropical mean LW flux anomalies are significant at the 95% level only for the Hadley Centre model at 0.6 and for the NCEP Reanalysis model at 0.3 (*19*). None of the models show significant correlations with the observed SW flux anomalies.

The seasonal model anomalies for 1993 through 1997 are shown for comparison in Fig. 3, averaged consistently with the observations. The models miss the semi-annual cycle in the SW flux anomalies after 1993, i.e., they are missing the observed seasonal cycle change in tropical albedo shown in Fig. 3.

We conclude that the large decadal variability of the LW and SW radiative fluxes shown in Figs. 1 through 3 appear to be caused by changes in both the annual average and seasonal tropical cloudiness. In general, these changes are not well predicted by current climate models, or by the NCEP Reanalysis. Indeed, current assessments (*1*) of global climate change have found clouds to be one of the weakest components in climate models. This leads to a threefold uncertainty in the predictions of the possible global warming over the next century. Though the models represent reasonably well the large regional shifts of convective cloudiness during an El Niño event, the current results indicate that the models are struggling to produce the more subtle, but still large, decadal changes seen in the radiation data. Three potential reasons for the disagreement are as follows: (i) The observed cloud and radiation changes are forced by SST changes, but the clouds in the models do not respond correctly to the forcing. Note that the SST forcing includes both global change as well as natural decadal variability such as the Arctic Oscillation and the Pacific Decadal Oscillation. (ii) The radiation budget and cloud fluctuations are forced by changes in the climate system other than SST. (iii) The radiation budget and cloud fluctuations are an unforced natural variability.

Independent evidence for decadal tropical change includes an observed increase in tropical mean temperature lapse rate, which is also not reproduced by climate models (*20*). The recent IPCC Climate Change report (*1*) indicates an increase in lapse rate beginning about 1991 [fig. 2.12 in (*1*)], coinciding with the rise in LW fluxes in Fig. 1. Our results are qualitatively consistent in that an increased LW flux will primarily increase atmospheric cooling, whereas a decrease in reflected solar will increase surface heating.

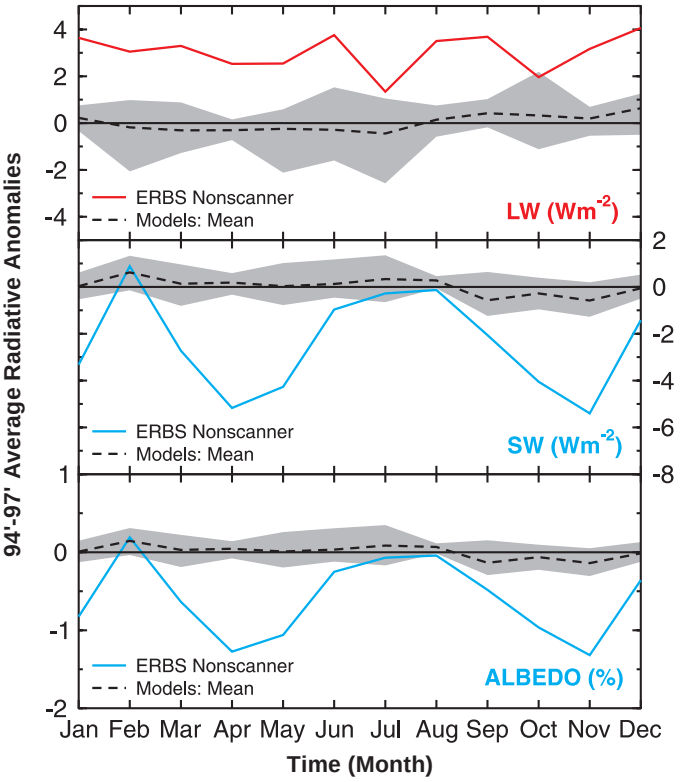

Fig. 3. Satellite record of the tropical mean (20°S to 20°N latitude) seasonal cycle of LW thermal emitted flux anomaly (top panel), SW flux anomaly (middle panel), and SW albedo anomaly (lower panel). Albedo is the fraction of solar radiation incident on Earth that is reflected back to space. The anomalies are averaged for the 1994 to 1997 period, which shows a large semi-annual cycle in the SW and net fluxes in Fig. 2. Anomaly results for the same 1994 to 1997 period from the climate model runs are shown as a dashed line (average of all models) and gray shading (total range of model results). Model runs are the same ones used in Fig. 4.

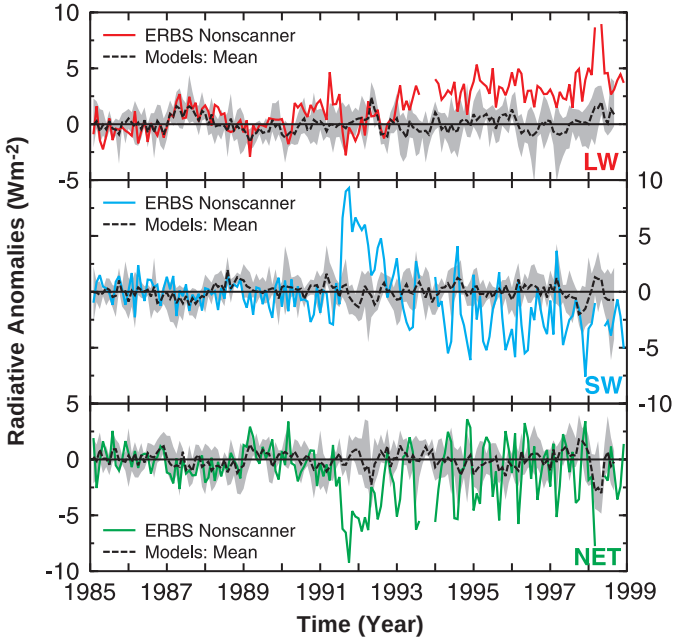

Fig. 4. Comparison of the observed broadband LW and SW flux anomalies for the tropics with climate model simulations using observed SST records. The models are not given volcanic aerosols, so they should not be expected to show the Mount Pinatubo eruption effects in mid-1991 through mid-1993. The dashed line shows the mean of all five models, and the gray band shows the total range of model anomalies (maximum to minimum).

However, we caution against interpreting the decadal variability as evidence of greenhouse gas warming. Whether the changes seen in the radiative balance in the last two decades are the result of natural variability or are a response to global change remains to be determined. A major step in understanding these changes is given in a companion paper in this issue (*21*), which offers a hypothesis for the link between these radiative balance changes and corresponding changes in the dynamical climate system, a system that appears to be much more variable than previously thought.

References and Notes

1. IPCC, *Climate 2001, The Scientific Basis*, J. T. Houghton *et al.* Eds. (Cambridge Univ. Press, Cambridge, 2001), pp. 87–91.
2. B. A. Wielicki *et al.*, *Bull. Am. Meteorol. Soc.* **76**, 2125 (1995).
3. B. A. Wielicki *et al.*, *Bull. Am. Meteorol. Soc.* **77**, 853 (1996).
4. The record of overlapping climate-quality satellite radiation data now extends from the Nimbus-7 mission, launched in 1978, through the current Earth Observing System Terra mission, launched in late 1999. Measurement of these fluxes in sufficient accuracy for climate research, however, is a serious challenge. Radiation fields vary greatly with spectral wavelength, time, latitude, longitude, and height from the surface of Earth; solar elevation angle; satellite viewing elevation angle; and satellite viewing azimuth angle relative to the solar plane (*2*). Achieving calibration accuracy of 1% or better as well as sufficient sampling of this eight-dimensional space is a major challenge to achieving data of climate accuracy of order 1 Wm^{-2}.
5. B. R. Barkstrom *et al.*, *Bull. Am. Meteorol. Soc.* **70**, 1254 (1989).
6. Nonscanning radiometers view the entire hemisphere of radiation but with a roughly 1000-km field of view. Scanning radiometers view radiance from a single direction and must estimate the hemispheric emission or reflection. Because of this fundamental difference, scanner and NS radiometers are each treated as a single group for the anomalies. For details on the radiometers and data sources used in this study, see (*19*).
7. P. Minnis *et al.*, *Science* **259**, 1411 (1993).
8. Narrowband atmospheric window and sounding instruments attempt to estimate the full broadband LW fluxes with the use of regressions and radiative modeling approaches. For results using the latest versions of these data sets, see (*19*).
9. The ERBS active cavity NS calibration record was examined for changes in instrument channel gains and offsets, for SW filter dome transmission loss over time, and for nonuniformity of dome transmission. The calibration uncertainties found were less than 0.5 Wm^{-2}, and the time variations in ERBS calibration were inconsistent with the tropical mean SW and LW flux anomalies in Figs. 1 through 4. For details, see (*19*).
10. T. Wong *et al.*, *J. Clim.* **13**, 4256 (2000).
11. There is no significant change in the ERBS spacecraft orbit during the record, so the sudden appearance of the semi-annual cycle after 1993 cannot be explained by diurnal cycle sampling errors causing seasonal cycle errors. The ERBS spacecraft orbit precesses through 12 hours of local time in approximately 36 days. Because Earth is viewed on both sides of the orbit 12 hours apart in the tropics, the full diurnal cycle is covered every 36 days or about 10 times per year. Diurnal cycle sampling errors across the tropics estimated by sub-sampling hourly geostationary data gave values of 0.14, 0.24, and 0.37 Wm^{-2} for LW fluxes from the TRMM, ERBS scanner, and ERBS NS data, respectively. The corresponding errors for SW fluxes are larger at 0.9, 1.6, and 1.7 Wm^{-2} (*22*, *23*). We conclude that large (5 Wm^{-2}) changes in seasonal cycle of tropical radiation have occurred in the decade of the 1990s.
12. SSTs were the NCEP/Reynolds reconstructed SSTs (*24*), except for the HadAM3 model, which used version 3.1 of the UK Met Office Global Sea Ice Coverage and Sea Surface Temperature (GISST). [experiments provided by and described in (*14*)].
13. V. D. Pope *et al.*, *Clim. Dyn.* **16**, 123 (2000).
14. D. M. H. Sexton *et al.*, *Clim. Dyn.* **17**, 669 (2001).
15. J. T. Kiehl *et al.*, *J. Clim.* **11**, 1131 (1998).
16. N. C. Lau, *J. Clim.*, **14** 2846 (2001).
17. C. T. Gordon *et al.*, *J. Clim.* **13**, 2239 (2000).
18. R. E. Kistler *et al.*, *Bull. Am. Meteorol. Soc.* **82**, 247 (2001).
19. Supplemental material is available on *Science* Online at www.sciencemag.org/cgi/content/full/295/5556/841/DC1.
20. D. J. Gaffen *et al.*, *Science* **287**, 1242 (2000).
21. J. Chen, B. W. Carlson, A. D. Del Genio, *Science* **295**, 838 (2002).
22. D. F. Young *et al.*, *J. Appl. Met.* **37**, 572 (1998).
23. T. Wong *et al.*, *AMS 12th Symposium on Global Change*, 14 to 18 January 2001, Albuquerque, NM (American Meteorological Society, Boston, 2001).
24. T. M. Smith *et al.*, *J. Clim.* **9**, 1403, (1996).
25. The Nimbus 7 satellite is in local noon orbit, which is highly biased for solar fluxes. The Scanner for Radiation Budget (ScaRaB)/Meteor satellite requires about 7 months to precess through the diurnal cycle, causing diurnal cycle sampling errors to occur in seasonal cycles. The ScaRaB/Resurs and CERES/Terra data are sun-synchronous satellites fixed at local sampling times near 10 to 11 a.m. Further research is required to achieve accurate diurnal cycle corrections for SW fluxes using these satellites.

26. We would like to thank the CERES science, algorithm, and data management teams, whose contributions were essential to continuing and improving this key climate radiation data set. The surprising initial TRMM CERES data was the motivation for this analysis. We would like to thank the NASA Langley Atmospheric Sciences Data Center for providing the ERBE S-4 and CERES ES-4 data sets. The NCEP–NCAR 50-Year Reanalysis data were obtained at http://wesley.wwb.noaa.gov/reanalysis.html. G. Gibson and D. Young provided reviews that greatly helped the clarity of the paper. R. B. Lee III, G. L. Smith, J. Paden, and K. Bush provided a careful review of the ERBS NS calibration record. Funding for this research was provided by the NASA Earth Sciences Enterprise. The work at the Hadley Centre was supported by the UK Department for Environment, Food and Rural Affairs under contract PECD/7/12/37.

29 August 2001; accepted 3 January 2002

Distinguishing Inchworm and Hand-Over-Hand Processive Kinesin Movement by Neck Rotation Measurements

Wei Hua,[1] Johnson Chung,[2] Jeff Gelles[1,2]*

The motor enzyme kinesin makes hundreds of unidirectional 8-nanometer steps without detaching from or freely sliding along the microtubule on which it moves. We investigated the kinesin stepping mechanism by immobilizing a *Drosophila* kinesin derivative through the carboxyl-terminal end of the neck coiled-coil domain and measuring orientations of microtubules moved by single enzyme molecules at submicromolar adenosine triphosphate concentrations. The kinesin-mediated microtubule-surface linkage was sufficiently torsionally stiff ($\geq 2.0 \pm 0.9 \times 10^{-20}$ Newton meters per radian^2) that stepping by the hypothesized symmetric hand-over-hand mechanism would produce 180° rotations of the microtubule relative to the immobilized kinesin neck. In fact, there were no rotations, a finding that is inconsistent with symmetric hand-over-hand movement. An alternative "inchworm" mechanism is consistent with our experimental results.

The motor enzyme kinesin moves membrane-bound organelles along microtubules in eukaryotic cells (*1*). Microtubule-based movements of organelles in vivo may be driven by as few as one motor enzyme molecule (*2*). Observations of the movement of single kinesin molecules in vitro demonstrate that the enzyme is well adapted to functioning as an isolated single molecule in living cells. First, the enzyme is processive: The kinesin undergoes multiple catalytic turnovers without detaching from the microtubule (*3*, *4*), facilitating efficient organelle transport over long distances (*5*). Second, the duty ratio of kinesin is high: The enzyme cannot freely slide in the direction of the microtubule axis during most or all of its enzymatic cycle (*6*, *7*) and thus is able to move forward even when opposed by the substantial elastic forces imposed by mechanical obstructions to organelle movements inside cells.

The mechanism by which single kinesin molecules achieve processive, high–duty-ratio movement is not well understood. Both of the enzyme's two identical head domains are required for such movement: the kinesin one–headed homolog KIF1A is processive but has low duty ratio (*8*–*10*), and truncated kinesin constructs with only one head have low duty

[1]Biophysics and Structural Biology Program, [2]Biochemistry Department, Brandeis University, Waltham, MA 02454–9110, USA.

*To whom correspondence should be addressed. E-mail: gelles@brandeis.edu